# Microfabrication, Assembly, and Hermetic Packaging of mm-Sized Free-Floating Neural Probes

P. Yeon, J.L. Gonzalez, M. Zia, S. Kochupurackal Rajan, G.S. May, M.S. Bakir, and M. Ghovanloo
School of Electrical and Computer Engineering, Georgia Institute of Technology, Atlanta, Georgia, U.S.A.

***Abstract*—In this paper, we present a new micromachining (MEMS) fabrication process, microassembly, and hermetic packaging of free-floating neural probes (<1 mm$^3$), wrapped with a bonding-wire coil for wireless power/data transmission and remote monitoring of hermetic sealing failure. The current prototype probe is a pushpin-shaped implantable device consisting of a mock-up integrated circuit (IC) that also serves as a substrate, stacked above a microfabricated silicon die with a ∅100 µm non-plated through-hole and embedded cavities to house small surface mount (SMD) capacitors. In center of the micromachined die, a ∅81 µm sharpened tungsten electrode is inserted and held upright in the through-hole. Except for the tip of the electrode, the device is coated with 5 µm thick parylene-C for hermetic sealing with an additional layer of Polydimethylsiloxane (PDMS) to improve biocompatibility. The bonding-wire wound coils are carefully characterized and compared with electromagnetic simulations. Variations in the Q-factor and resonance frequency, which affect power/data transmission performance have been examined across 12 samples in terms of phase-dip amplitude, which corresponds to failure in hermetic sealing.**

***Keywords*—Free-floating wireless implantable neural recording, biocompatibility, distributed neural interfacing, micromachining, hermetic packaging, inductive link.***

## I. Introduction

The ability to record and analyze neural signals over a large area of the brain, simultaneously, allow brain machine interfaces (BMIs) to restore sensory and motor abilities in patients suffering from such deficits, caused by traumatic injuries, neurological diseases, or loss of limbs. This is also a motivation behind development of advanced tools for understanding the underlying mechanisms behind many neurological disorders. To obtain useful clinical data from invasive BMIs and neuroscience tools, neural interfacing devices are required to overcome the major hurdle of obtaining long-term and stable recordings for large populations of neurons throughout the brain areas of interest [1]. Several implantable neural interfacing devices have been developed in recent years [2], [3]. Even though the demonstrated neural recording implants are clinically viable and eliminate tethering effects by integrating wireless data and power transfer features, they fall short of achieving long-term, stable recordings from sufficiently large neural populations because of limited brain area coverage. They also suffer from scar formation due to large device sizes that result in signal-to-noise ratio (SNR) degradation and shortened BMI lifetime [4].

Free-floating mm-sized neural probes distributed across the large brain area can replace the bulky, localized, and sometimes anchored neural recording implants [5]. Tens to hundreds of free-floating ~1 mm$^2$ sized probes, surrounded by a resonator coil and placed in a subcortical layer above a brain region of interest, can transmit the recorded neural signal outward from a human head while being powered through a shared 3-coil inductive link as depicted in Fig. 1 [6]. To take the distributed free-floating neural recording system from concept to a clinically viable system, there are several major challenges: 1) application-specific integrated circuit (ASIC) design with an extremely low power budget and size constraints, 2) wireless power/data transmission for multiple mm-sized implants, 3) back-end signal processing, 4) MEMS fabrication/assembly, 5) biocompatible hermetic packaging, and 6) neurosurgical procedure. In this paper, we focus on the MEMS fabrication/assembly and biocompatible hermetic packaging of these mm-sized neural probes. For long-term monitoring, the neural probe design must be concrete, hermetically sealed, and biocompatible to avoid three major failure mechanisms of the neural probes: biological, material, and mechanical [7]. Mechanical design and hermetic packaging aspects of the probes are highly entangled, and need to be addressed together while considering the other abovementioned challenges. Obviously, the mechanical design should be physically robust to withstand handling and insertion, while materials used in packaging should undergo hermeticity testing before implantation even in animal subjects.

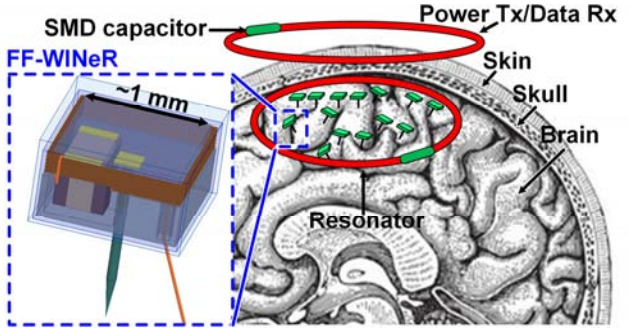


Fig. 1. Conceptual rendering of distributed mm-sized free-floating wireless implantable neural recording system (FF-WINeR) encompassed by a high-Q resonator that relays power and data from/to the external power transmitter (Tx) and data receiver (Rx), respectively.

The mechanical design of our 1-mm$^2$ free-floating wireless implantable neural recording (FF-WINeR) "pushpin" probe was first introduced, along with its manual hermetic packaging failure testing, in [5]. That design placed significant burden on the area-constrained ASIC die by requiring about 4% of the available silicon real estate set aside for formation of a through-silicon hole (TSH), right in the middle of the die to pass the microwire electrode(s). This can also significantly increase the

This work was supported in part by the National Science Foundation under awards ECCS-1408318 and ECCS-1407880.

978-1-5090-5803-7/17/$31.00 ©2017 IEEE

cost and reduce the yield of developing prototypes when the required microfabrication steps need to be done at the die level, as opposed to wafer level.

In the new FF-WINeR mechanical/microassembly design, proposed here, we have developed a micromachined die that supports all passive components of the probe, and eventually flip-chip bonds onto the ASIC, isolating the costly ASIC from the wafer-level MEMS fabrication steps. We have fabricated a passive silicon die with a TSH for the tungsten electrode(s) to pass through, and etched areas reserved for surface mounted device (SMD) capacitors in order to minimize the impact on the overall size of the probe. We have also envisioned a high-Q MEMS receiver (Rx) coil to be embedded in the passive die for batch fabrication. However, in the current prototype, a bonding-wire coil is wrapped around a mockup active die to characterize the effects of the micromachined die over the coil, packaging, electrical parameters, and sample-to-sample variations. Section II presents the proposed new FF-WINeR fabrication process. Section III describes the electromagnetic simulation and measurement setup, and results of characterizing the bonding-wire coil in the presence of micromachined dice, packaging, and tissue media, followed by the concluding remarks.

## II. Microfabrication and Assembly Process

The new FF-WINeR consists of an active Si die housing a wirelessly-powered ASIC for recording and transmitting neural signals and a passive Si die providing mechanical support for the neural probe(s). In the current prototype, dummy active die was fabricated with metal pads for connecting the wire-wound Rx coil, SMD capacitors, penetrating tungsten electrode, and a soft reference electrode. The fabrication process involves forming a Si dioxide passivation layer on top of a Si wafer, followed by metallization and lift-off to create the contact pads. E-beam evaporation was used to deposit a Ti adhesive layer, a Cu layer for reduced pad resistance, and a gold passivation layer on top.

Through-silicon cavities were pattered and etched on the passive Si die using a BOSCH process to anchor the tungsten and reference electrodes, and also to protect the SMD capacitors. A large metal pad was deposited around the center ∅100 µm TSH on the passive Si die to prevent the spread of conductive epoxy or soldering paste beyond the pad during the reflow process to keep it at the center of the passive die and in contact with the main electrode. Figs. 2a and 2b show the fabricated mockup active and passive dice, respectively.

The prototype mockup FF-WINeR is assembled through the procedure shown in Fig. 2c, which begins by winding a 6-turn coil around the 1.05 × 1.05 × 0.3 mm$^3$ mockup active Si die, using an insulated bonding-wire (Microbonds, Canada) with 25 µm gold conductor diameter. Two ends of the coil are connected to the Ti/Cu/Au pads by an ultrasonic wire-bonding machine. Detailed design, fabrication, and characterization of the bonding-wire wound coils are described in [5], [6]. Conductive epoxy was applied on the metal pads, reserved for two SMD capacitors (0201 and 01005) one Rx coil tuning and other for ripple-rejection, which are too large to be integrated on chip, are mounted on the metal pads, and the epoxy is cured at 65-121 °C for 5-10 minutes. The conductive epoxy is applied again on the metal pads reserved for electrodes. The passive Si die is aligned and glued on top of the mockup active Si die. The tungsten microelectrode, which is 81 µm in diameter, including its 3 µm

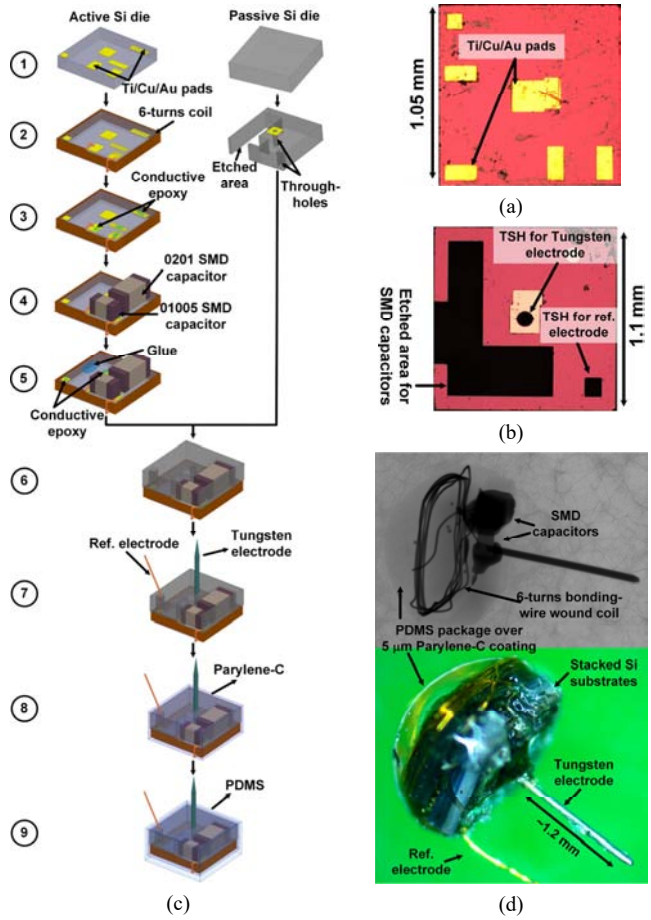


Fig. 2. (a) Mockup active silicon die with pads for SMD capacitors. (b) Micromachined passive die. (c) Microassembly procedure of the mm-sized free-floating neural probe: (1) Active and passive dice, (2) winding bonding-wire Rx coil around the active die, (3) applying conductive epoxy, (4) placing SMD capacitors, (5) applying conductive epoxy and glue, (6) stacking and aligning the Si dice, (7) inserting electrodes into TSHs, (8) coating the device with parylene-C, (9) coating the device with PDMS. (d) X-ray image (top) and micrograph of the mockup FF-WINeR probe.

thick Teflon insulation (Microprobes, Gaithersburg, MD) in this prototype, is cut at a desired length, depending on the target brain layer/structure to record from, and inserted through the ∅100 µm TSH in the middle of the passive Si die, and electrically connects to the center pad of the active Si die when the conductive epoxy is cured. Similarly, a piece of bonding-wire is inserted through the TSH on the corner, for the reference electrode, and connected to the associated pad on the active die. For hermetic packaging, the assembled device is coated with 5 µm thick Parylene-C by vapor deposition (SCS Labcoater 2 PDS 2010, Specialty Coating Systems, Indianapolis, IN). The device is then coated with an additional layer of PDMS (Sylgard 184, Dow Corning, Midland, MI) for physical protection, smoothing, improving life-span, and biocompatibility of the free-floating probe. An X-ray image and microphotograph of the new mockup FF-WINeR prototype are shown in Fig. 2d.

## III. Simulation and Measurement Results

A realistic model was constructed to optimize geometries of the bonding-wire wound Rx coil of the FF-WINeR probe

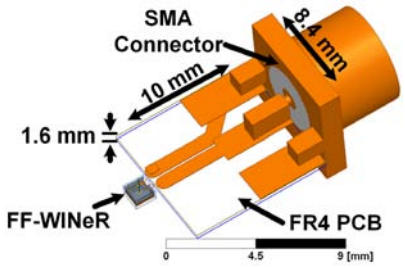


Fig. 3. HFSS simulation model for the FF-WINeR on a FR4 PCB, including details of its interconnection with a VNA via a SMA connector.

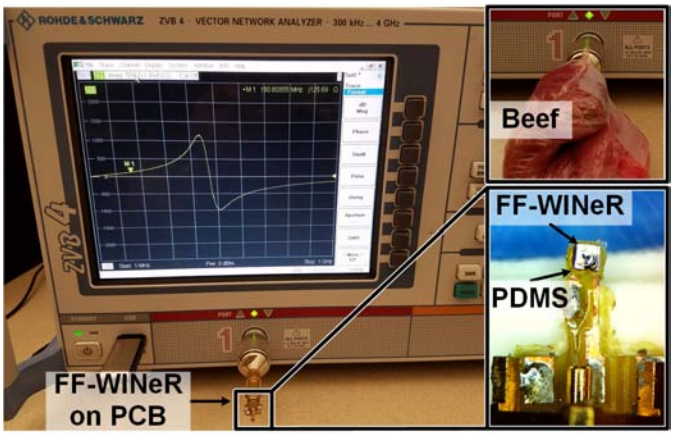


Fig. 4. Experiment setup used to characterize the bonding-wire coil fabricated around the FF-WINeR on a FR4 PCB that forms the interconnect between the FF-WINeR and VNA via a SMA connector. Upper right inset: FF-WINeR wrapped in a ~1 cm thick layer of beef to mimic the lossy tissue media. Lower right inset: Close-up view of the FF-WINeR Rx coil, packaged in the PDMS and mounted on a small PCB, which is soldered to the SMA connector.

in presence of the micromachined dice, polymer packaging, and tissue media in the High Frequency Structural Simulator (HFSS) environment (ANSYS, Canonsburg, PA), as shown in Fig. 3. The coil is mounted on a 8.4 × 10 × 1.6 $mm^3$ 2-layer printed circuit board (PCB), made of FR4, via bonding-wires. The PCB layout was also exported to HFSS, to model interconnection between the FF-WINeR and a vector network analyzer (VNA) via SMA connector. The inductance, resistance, and Q-factor of the Rx coil are simulated using this model to be compared with corresponding experimental data. The optimization procedure has been explained in [6], and will not be repeated here.

Fig. 4 shows the experimental setup, using which the 6-turn bonding-wire Rx coil around the fabricated mock FF-WINeR probe was characterized in air and lossy tissue media. The latter was created by wrapping a ~1 cm thick layer of beef around the FF-WINeR, as shown in Fig. 4 upper right inset. Fig. 4 lower right inset shows a close up view of the Rx coil in the assembled FF-WINeR mock up, mounted on a T-shaped PCB. To improve the measurement accuracy, we used the de-embedding method in [8] to compensate for the parasitic effects of the interconnects, which are considerably larger than the FF-WINeR Rx coil, as shown in Figs. 3 and 4. In this process, the Z-parameters of an identical short-circuited PCB and the Y-parameters of an identical open-circuited PCB are subtracted from the measured data from the actual probe (in both air and tissue media) to eliminate the parasitic resistance/inductance and capacitance of the interconnects, respectively.

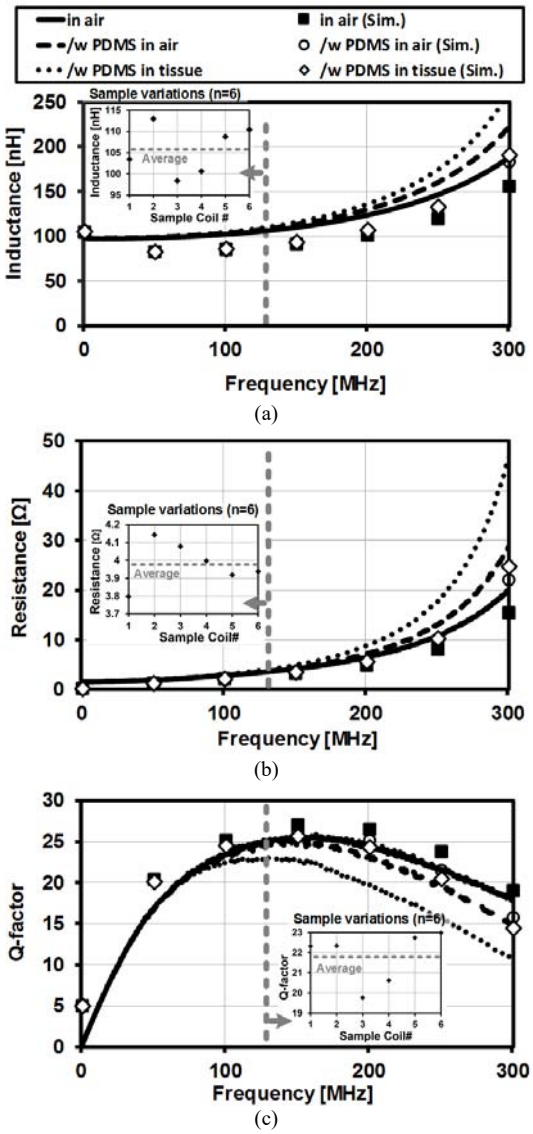


Fig. 5. HFSS-simulated and measured (a) inductance, (b) resistance, and (c) Q-factor of the bonding-wire Rx coil, wound around the FF-WINeR, in air with no coating, polymer coating in air, and polymer coating in tissue media. Insets: (a) inductance, (b) resistance, and (c) Q-factor variations among 6 fabricated samples coated with parylene and PDMS in the tissue media.

Fig. 5 shows the simulated and measured results of inductance, resistance, and Q-factor for the 6-turn bonding-wire Rx coil wound around the mock up FF-WINeR core, made up of the mock-up active and passive Si dice, SMD capacitors, and tungsten electrode. To study variations among hand-made prototypes, six samples were measured in air before coating, with coating in air, and with coating in the beef tissue media. It can be seen that the measurement results are in good agreement with the HFSS simulation results in air. However, the gap between simulation and measurement results becomes wider in the tissue media, perhaps because of the difference in material properties of the homogeneous tissue in the HFSS model, and irregular geometry of the beef layer in measurement setup.

The inductance and resistance of the Rx coil, coated with parylene and PDMS in the air and tissue media increase faster than those in air vs. frequency, particularly above 100 MHz.

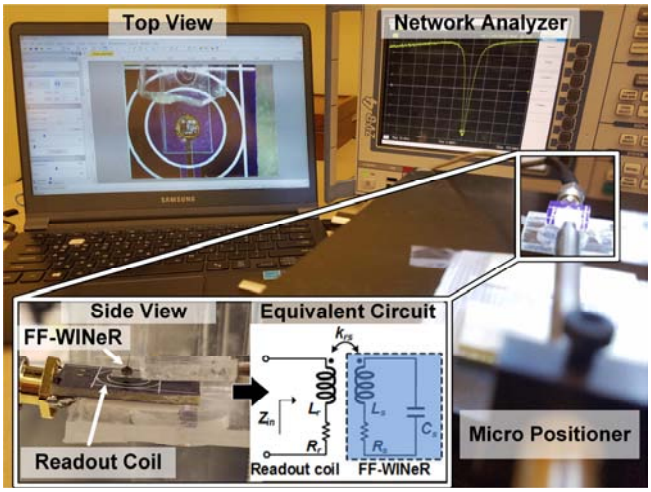


Fig. 6. Measurement setup to wirelessly monitor the resonant frequency, $f_0$, of FF-WINeR prototypes. Insets: side view (left), and equivalent circuit (right) of a wireless sensing inductive link to measure $f_0$ of the hermetically sealed FF-WINeR Rx LC-tank.

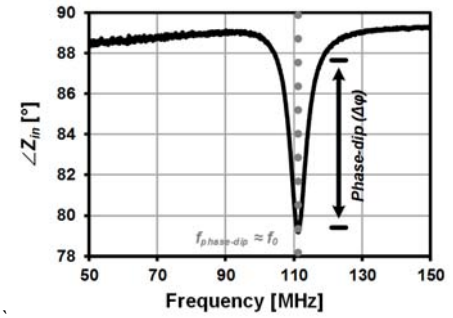


(a)

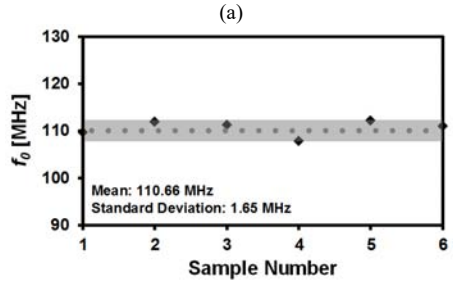


(b)

Fig. 7. (a) Measured input impedance phase ($\angle Z_{in}$) through a readout coil vs. frequency. (b) Resonant frequency variations among 6 FF-WINeR samples.

For example, from 100 MHz to 130 MHz, the inductance and resistance of the packaged coil in air are increased by 1.72% and 3.08%, respectively, and those in the tissue media by 3.52% and 12.4%, respectively, indicating that the resistance increases faster than the inductance, both in polymer and tissue media, resulting in a drop in the Q-factor. This is the result of lowered self-resonant frequency of the Rx coil because of the higher permittivity and loss tangent of coating and tissue media. In terms of variability among 6 samples, Fig. 5 insets show the average inductance, resistance, and Q-factor to be 105.7 ± 5.8 nH, 3.98 ± 0.12 Ω, and 21.8 ± 1.3, respectively.

Fig. 6 shows the experiment setup to wirelessly measure the resonant frequency, $f_0$, of the hermetically sealed mock up FF-WINeR by monitoring changes in the phase of input impedance, $\angle Z_{in}$, of a readout coil, $L_r$, aligned with and weakly coupled to the Rx coil ($L_sC_s$). Changes in $f_0$ can be an indicator of possible leaks in the hermetic sealing. The FF-WINeR is placed on a Plexiglas sheet that is moved by an X-Y micro-positioner to be accurately align 0.5 mm above the readout coil. Fig. 7a shows the measured $\angle Z_{in}$ for a FF-WINeR prototype vs. frequency. It can be shown that the frequency of the phase-dip, $\Delta\varphi = \tan^{-1}(k_{rs}^2 Q_s)$, is equal to $f_0$ due to weak coupling ($k_{rs} \approx 0.091$ from HFSS simulation) and high Q-factor ($Q_s \sim 21.8$) of the Rx coil [9]. The measured $f_0$ for 6 FF-WINeR samples are plotted in Fig. 7b, where the mean and standard deviation of $f_0$ are 110.66 ± 1.65 MHz, with the Rx coil connected to a 20 pF 01005 SMD capacitor from Murata (Kyoto, Japan) with ±5% tolerance.

## IV. Conclusion

Microfabrication, assembly, and packaging of a free-floating wireless integrated neural recording (FF-WINeR) probe that occupies less than 1 mm$^3$ in volume is presented. To facilitate fabrication, particularly when costly FF-WINeR ASIC prototypes are only available at the die level, improve the mechanical robustness, and increase yield, a micromachined passive die with TSHs for electrodes and etched spaces for SMD capacitors have been added to the device architecture. A multifunction coil, wrapped around the FF-WINeR using bonding wires for receiving power, transmitting data, and monitoring the hermetic sealing integrity was characterized by constructing a realistic simulation model in HFSS and comparison with measurements. Fabrication tolerances in the $f_0$ (100-120 MHz nominal value) can be compensated using auto-resonance tuning [10].

## References


[1] M. A. Lebedev, *et al*., "Future developments in brain-machine interface research," *Clinics*, vol. 66, supl. 1, pp. 25-32, June 2011.

[2] M. Yin, D. A. Borton, J. Aceros, W. R. Patterson and A. V. Nurmikko, "A 100-channel hermetically sealed implantable device for chronic wireless neurosensing applications," *IEEE Trans. Biomed. Circuits Syst.*, vol. 7, no. 2, pp. 115-128, Apr. 2013.

[3] R. Muller, H. P. Le, W. Li, P. Ledochowitsch, S. Gambini, T. Bjorninen, A. Koralek, J. M. Carmena, M. M. Maharbiz, E. Alon, J. M. Rabaey, "A minimally invasive 64-channel wireless μECoG implant," *IEEE J. Solid-State Circuits*, vol. 50, no. 1, Jan. 2015.

[4] J. Tuner, W. Shain, D. Szarowski, M. Anderson, S. Martins, M. Isaacson, and H. Craighead, "Cerebral astrocyte response to micromachined silicon implants," *Experimental neurology*, vol. 156, no. 1, pp. 33-49, Mar. 1999.

[5] P. Yeon, S. A. Mirbozorgi, B. Ash, H. Eckhardt, and M. Ghovanloo, "Fabrication and microassembly of a mm-sized floating probe for a distributed wireless neural interface," *Micromachines*, vol. 7, no. 9, p. 154, Sep. 2016.

[6] P. Yeon, A. Mirbozorgi, and M. Ghovanloo, "Optimal design of a 3-coil inductive link for millimeter-sized biomedical implants," *Proc. IEEE Biomed. Circuits Syst. Conf. (BioCAS)*, pp. 396-399, Oct. 2016.

[7] J. C. Barrese, N. Rao, K. Paroo, C. Triebwasser, C. V-. Irwin, L. Franquemont, and J. P. Donoghue, "Failure mode analysis of silicon-based intracortical microelectrode arrays in non-human primates," *J. Neural Eng*., vol. 10, no. 6, Nov. 2013, Art. ID 066014.

[8] D. Ahn and M. Ghovanloo, "Optimal design of wireless power transmission links for millimeter-sized biomedical implants," *IEEE Trans. Biomed. Circuits. Syst*., vol. 10, no. 1, pp. 125-137, Feb. 2016.

[9] Q.-A. Huang, L. Dong, and L.-F. Wang, "LC passive wireless sensors toward a wireless sensing platform: status, prospects, and challenges," *IEEE J. Microelectromech. Syst*., vol. 25, no. 5, pp. 822-841, Sep. 2016.

[10] B. Lee, P. Yeon, and M. Ghovanloo, "A multicycle Q-modulation for dynamic optimization of inductive links," *IEEE Trans. Ind. Electron*., vol. 63, no. 8, pp. 5091-5100, Aug. 2016.